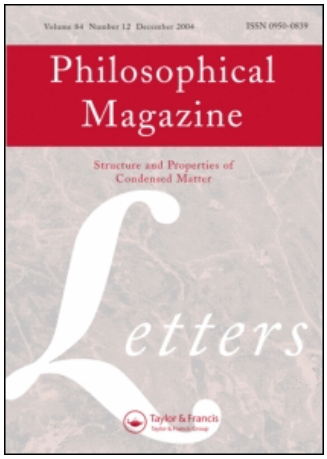

Philosophical Magazine Letters
Publication details, including instructions for authors and subscription information:
http://www.informaworld.com/smpp/title~content=t713695410

Diffuse-interface description of grain boundary motion

DANAN FAN; LONG-QING CHEN

To cite this Article: DANAN FAN and LONG-QING CHEN , 'Diffuse-interface description of grain boundary motion', Philosophical Magazine Letters, 75:4, 187 - 196
To link to this article: DOI: 10.1080/095008397179615
URL: http://dx.doi.org/10.1080/095008397179615

PHILOSOPHICAL MAGAZINE LETTERS, 1997, VOL. 75, NO. 4, 187–196

Diffuse-interface description of grain boundary motion

By DANAN FAN and LONG-QING CHEN

Department of Materials Science and Engineering, The Pennsylvania State University, University Park, PA 16802, USA

[*Received in final form 11 December 1996 and accepted 20 January 1997*]

ABSTRACT

A diffuse-interface kinetic field model for describing grain boundary motion is proposed. It is based on the time-dependent Ginzburg–Landau equations, in which grain orientations are described by non-conserved order parameters. A simple example, a two-dimensional circular grain boundary with isotropic grain boundary energy, is considered. It is shown that, in the sharp-interface limit, the boundary migration velocity does not explicitly depend on the magnitude of grain boundary energy, and is linearly proportional to its mean curvature. Our numerical simulations demonstrated that, even for a boundary with a finite thickness, its migration velocity is also proportional to the mean curvature, which is, surprisingly, insensitive to the accuracy of the numerical method, although the values for the boundary velocity match the sharp-interface solution only if there are enough grid points to resolve the boundary region in the simulation. The applicability of the diffuse-interface model to simulating microstructural evolution and grain growth kinetics is discussed.

§ 1. INTRODUCTION

Grain boundary migration takes place in polycrystalline materials to reduce the total excess free energy associated with them, a process usually referred to as grain growth. Most of previous mean-field and statistical theories as well as computer simulation models for grain growth were reviewed by Atkinson (1988), Glazier (1990) and Fradkov (1993). Essentially all these models are based on the sharp-interface model of grain boundaries, which describes grain boundaries as abstract geometrical surfaces possessing properties such as area, curvature, free energy, and mobility. Recently, we proposed a rather different model for investigating grain growth kinetics (Chen 1995, Chen and Yang, 1994, Fan 1996, Fan and Chen 1997). A key new feature of this model is that the grain boundaries are diffuse with a finite thickness, similar to the theoretical treatment of antiphase domain boundaries by Allen and Cahn (1979). The grain boundary energy is automatically introduced through the gradient energy terms in the free energy functional. One of the main advantages of this model is that an arbitrary microstructure can be easily treated since the interfaces are not singular surfaces requiring imposition of moving boundary conditions as in the sharp-interface description, but just a region where the fields have high gradients. The main purpose of this letter is to discuss the relationship between the sharp- and diffuse-interface descriptions for the motion of a grain boundary and the validity of the diffuse-interface field model in describing curvature-driven microstructural evolution. A particular example, the shrinking of a circular grain boundary with isotropic grain boundary energy in two dimensions, will be considered.

0950–0839/97 $12 · 00

§ 2. Diffuse-interface description of a grain boundary

In the diffuse-interface field model, a grain, with an arbitrary orientation in space, is described by a continuous field variable $\eta(r)$, and hence a grain boundary separating two grains can be described by two field variables, $\eta_1(r)$ and $\eta_2(r)$. The total free energy of an inhomogeneous system with a grain boundary can be written as:

$$F = \int \left[f_0(\eta_1(r), \eta_2(r)) + \frac{\kappa_1}{2}(\nabla \eta_1(r))^2 + \frac{\kappa_2}{2}(\nabla \eta_2(r))^2 \right] \mathrm{d}^3 r, \tag{1}$$

where $\nabla\eta_1$ and $\nabla\eta_2$ are the gradients of $\eta_1(r)$ and $\eta_2(r)$, f_0 is the local free energy density, and κ_1 and κ_2 are the gradient energy coefficients. The energy of a flat grain boundary between grain 1 and 2, σ_{gb}, can be calculated as

$$\sigma_{gb} = \int_{-\infty}^{+\infty} \left[\Delta f_0(\eta_1, \eta_2) + \frac{\kappa_1}{2}\left(\frac{\mathrm{d}\eta_1}{\mathrm{d}x}\right)^2 + \frac{\kappa_2}{2}\left(\frac{\mathrm{d}\eta_2}{\mathrm{d}x}\right)^2 \right] \mathrm{d}x. \tag{2}$$

For a flat boundary, the equilibrium profiles of $\eta_1(r)$ and $\eta_2(r)$ across the boundary may be obtained by solving the following Euler equations:

$$\frac{\partial \Delta f_0}{\partial \eta_1} = \kappa_1 \frac{\mathrm{d}^2 \eta_1}{\mathrm{d}x^2}, \tag{3 a}$$

$$\frac{\partial \Delta f_0}{\partial \eta_2} = \kappa_2 \frac{\mathrm{d}^2 \eta_2}{\mathrm{d}x^2}, \tag{3 b}$$

where $\Delta f_0(\eta_1, \eta_2)$ is the excess free energy density of an inhomogeneous system over an homogeneous system with equilibrium values of $\eta_1(r)$ and $\eta_2(r)$. Taking into account eqns (3 *a*) and (3 *b*), we have

$$\sigma_{gb} = \int_{-\infty}^{\infty} 2\Delta f_0 \, \mathrm{d}x = \int_{-\infty}^{\infty} \left(\kappa_1 \left(\frac{\mathrm{d}\eta_1}{\mathrm{d}x}\right)^2 + \kappa_2 \left(\frac{\mathrm{d}\eta_2}{\mathrm{d}x}\right)^2 \right) \mathrm{d}x. \tag{4}$$

If $\kappa_1 \neq \kappa_2$, it is not trivial to derive a closed analytical expression for the dependence of grain boundary width on the gradient coefficients κ_i. However, for $\kappa_1 = \kappa_2 = \kappa$, it can be easily shown that grain boundary width

$$l = \eta_q \left(\frac{\kappa}{\Delta f_0} \right)^{1/2}. \tag{5}$$

§ 3. Motion of a sharp grain boundary

Since the field variables describing the orientations of grains are non-conserved quantities, their spatial and temporal evolution of orientation field variables is described by the time-dependent Ginzburg–Landau equations,

$$\frac{\mathrm{d}\eta(r,t)}{\mathrm{d}t} = -L_i \frac{\delta F}{\delta \eta(r,t)}, \quad i = 1,2, \tag{6}$$

where L_i are the kinetic coefficients, t is time, and F is total free energy given in eqn. (1). Following the theoretical analysis of Allen and Cahn (1979) for antiphase domain boundaries, the derivation of the motion law for a more general sharp grain boundary in three dimensions is rather straightforward; however, for simplicity and

for comparison with numerical simulation results, we will consider the particular case of a circular grain embedded in another grain. In this case, we may employ the polar coordinates in two dimensions and substituting eqn. (1) into eqn. (6), one gets

$$\frac{1}{L_1}\frac{\partial \eta_1}{\partial t} = \kappa_1\left[\frac{\partial^2 \eta_1}{\partial r^2} + \frac{1}{r}\frac{\partial \eta_1}{\partial r}\right] - \frac{\partial f_0}{\partial \eta_1}, \tag{7 a}$$

$$\frac{1}{L_2}\frac{\partial \eta_2}{\partial t} = \kappa_2\left[\frac{\partial^2 \eta_2}{\partial r^2} + \frac{1}{r}\frac{\partial \eta_2}{\partial r}\right] - \frac{\partial f_0}{\partial \eta_2}. \tag{7 b}$$

Here, the orientation field variables (η_1, η_2) are the functions of position r and time t. The velocity at a constant η surface at the grain boundary is given by (Allen and Cahn 1979)

$$v = \left(\frac{\partial r}{\partial t}\right)_\eta = -\left(\frac{\partial \eta}{\partial t}\right)_r \Big/ \left(\frac{\partial \eta}{\partial r}\right)_t. \tag{8}$$

Substitute this expression into equation (7),

$$-\frac{v}{L_1}\frac{\partial \eta_1}{\partial r} = \kappa_1\frac{\partial^2 \eta_1}{\partial r^2} + \frac{\kappa_1}{r}\frac{\partial \eta_1}{\partial r} - \frac{\partial f_0}{\partial \eta} \tag{9 a}$$

$$-\frac{v}{L_2}\frac{\partial \eta_2}{\partial r} = \kappa_2\frac{\partial^2 \eta_2}{\partial r^2} + \frac{\kappa_2}{r}\frac{\partial \eta_2}{\partial r} - \frac{\partial f_0}{\partial \eta_2}. \tag{9 b}$$

In order to obtain a simple analytical solution, we assume $\kappa_1 = \kappa_2 = \kappa$ and the radius R of the circular grain is much greater than the grain boundary thickness ($R \gg l$). We multiply eqn. (9 *a*) by $\partial\eta_1/\partial r$ and eqn. (9 *b*) by $\partial\eta_2/\partial r$, and integrate both equations from $0 < r < \infty$, employing the following boundary conditions:

$$\partial\eta_1/\partial r = \partial\eta_2/\partial r = 0,\ \eta_1 = \eta_{1eq},\ \eta_2 = 0, \qquad \text{at } r = 0,$$
$$\partial\eta_1/\partial r = \partial\eta_2/\partial r = 0,\ \eta_2 = \eta_{2eq},\ \eta_1 = 0, \qquad \text{at } r = \infty,$$

and noticing that $f_0(\eta_{1eq}, 0) = f_0(0, \eta_{2eq})$, and $\partial\eta_1/\partial r$ and $\partial\eta_2/\partial r$ are not zero only around the grain boundary region, we have

$$-\left(\frac{v}{L_1} + \frac{v}{L_2}\right) = \frac{2\kappa}{R}. \tag{10}$$

Therefore, the velocity of a circular sharp grain boundary is

$$v = \frac{\mathrm{d}R}{\mathrm{d}t} = -\frac{2L_1L_2}{L_1 + L_2}\kappa\frac{1}{R} \tag{11}$$

which shows that the boundary velocity is linearly proportional to the mean curvature, $1/R$. It can also be seen from eqn. (11) that the boundary velocity is independent of the local free energy density f_0, and more surprisingly, independent of the grain boundary energy σ_{gb}. However, the result is consistent with the Allen–Cahn prediction on the motion of an antiphase domain boundary (Allen and Cahn 1979). The fact that the boundary velocity is independent of its energy while the driving force for its motion is proportional to its energy has been elegantly discussed by Bray (1994).

The dependence of the radius R on t is, then,

$$R_0^2 - R^2 = \frac{4L_1L_2}{L_1 + L_2}\kappa t. \tag{12}$$

An immediate result from eqn. (12) is that a circular grain with a sharp boundary will shrink following a power law with $m = 2$. If $L_1 = L_2 = L$, eqn. (12) is reduced to

$$R_0^2 - R^2 = 2Lkt. \tag{13}$$

§ 4. Numerical simulations

According to eqns. (11) and (5), the velocity of a sharp-interface grain boundary with isotropic grain boundary energy is linearly proportional to the mean curvature, and dependent on the coefficients κ_i and L_i, but not on Δf_0, whereas its thickness and grain boundary energy vary with κ_i and Δf_0. Therefore, varying Δf_0 while keeping κ_i and L_i constant will change the boundary energy and thickness but not its velocity. However, eqn. (11) was derived based on the assumption that the grain size is much larger than the boundary width, i.e. the sharp-interface limit. Meanwhile, in computer simulation of grain growth using a uniform grid for discretizing the differential eqns. (6), the condition $R \gg l$ is usually not satisfied. Therefore, it is important to understand the relationship between the numerical simulation based on the diffuse-interface description and its sharp-interface limit, the behaviour of a diffuse-boundary with finite thickness and, therefore, the validity of the diffuse-interface model in describing grain growth kinetics.

To simulate the grain boundary motion, we again consider a circular grain (η) embedded in another grain (η_1). We assumed a simple free energy density function,

$$f_0(\eta, \eta_1) = \sum_{i=1}^{2}\left(-\frac{\alpha}{2}\eta_i^2 + \frac{\beta}{4}\eta_i^4\right) + \gamma\eta_i^2\eta_1^2, \tag{14}$$

where α, β and γ are phenomenological parameters. It can be shown that, if $\gamma > \beta/2$, eqn. (14) gives four potential minima (wells) located at $(\eta, \eta_1) = (1, 0)$, $(-1, 0)$, $(0, 1)$, $(0, -1)$, which represent the equilibrium free energies of crystalline grains in four different orientations.

In the computer simulation, eqns. (6) are discretized in space and time. The Laplacian is discretized by

$$\nabla^2\eta = \frac{1}{(\Delta x)^2}\left[\frac{1}{2}\sum_j(\eta_j - \eta) + \frac{1}{4}\sum_k(\eta_k - \eta)\right], \tag{15}$$

where Δx is the grid size, j represents the first-nearest neighbours of site i, and k represents the second-nearest neighbours of site i. For discretization with respect to time, the explicit Euler equation is used:

$$\eta(t + \Delta t) = \eta(t) + \frac{\mathrm{d}\eta}{\mathrm{d}t}\Delta t, \tag{16}$$

where Δt is the time step for integration. In this paper, we employed 200×200 square lattice points to spatially discretize the kinetic equations with periodic boundary conditions applied along both Cartesian coordinate axes. The discretizing grid size Δx is chosen to be 2·0 and the time step Δt is 0·25.

We first consider the case $k_1 = k_2 = k = 2{\cdot}0$ and $L_1 = L_2 = L = 1{\cdot}0$, which gives an isotropic grain boundary energy and isotropic grain boundary mobility, respec-

tively. For the local free energy density function, the following initial parameters were assumed: $\alpha = 1{\cdot}0$, $\beta = 1{\cdot}0$ and $\gamma = 1{\cdot}0$. To vary Δf_0, the local free energy density function f_0 was multiplied by a coefficient μ. The width and energy of the grain boundary vary with μ while the velocity in the sharp-interface limit should not be affected. The initial radius of the circular grain was chosen as 120 grid points in diameter, which is much greater than the width of the grain boundary.

The temporal evolution of a circular grain for $\mu = 1{\cdot}0$ was shown in fig. 1 and the time dependences of the grain area for different values of μ are shown in fig. 2. The solid line in fig. 2 is the analytical solution described by eqn. (16). Decreasing μ reduces Δf_0, and hence increases the width of the grain boundary according to eqn. (5). It is shown that a circular grain with a narrower boundary (fig. 2) shrinks more slowly than that with a thicker boundary, i.e. the kinetic coefficient k increases with the boundary width. However, for all cases, the areas of the circular grain decrease linearly with respect to time, i.e. $R_t^2 - R_0^2 = kt$, so the boundary velocity is linearly proportional to the mean curvature. Moreover, although there is a significant change in k when μ decreases from 1·0 to 0·5, there is almost no change when μ decreases further, e.g. from 0·25 to 0·125. Equivalently, we can also examine the variation of grain radius with different μ as shown in fig. 3. The velocity v at a given time step $(v = \mathrm{d}R/\mathrm{d}t)$ is the slope of the R against t plot. It is clear that the grain boundary position and velocity differ significantly from those predicted by the sharp boundary approximation if there are not enough grid points to resolve the boundary region ($\mu = 1{\cdot}0$). However, for $\mu = 0{\cdot}125$, for which the thickness of the grain

Fig. 1

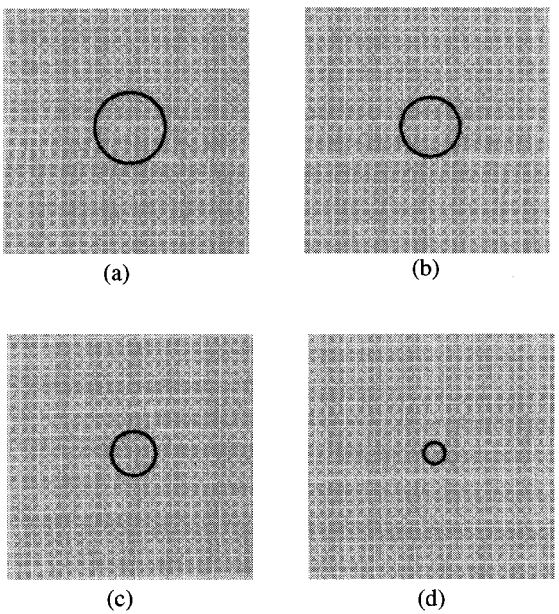

The temporal evolution of a circular grain embedded in another grain. (*a*) Time step= 1000; (*b*) time step= 3000; (*c*) time step= 5000, (*d*) time step= 7000.

Fig. 2

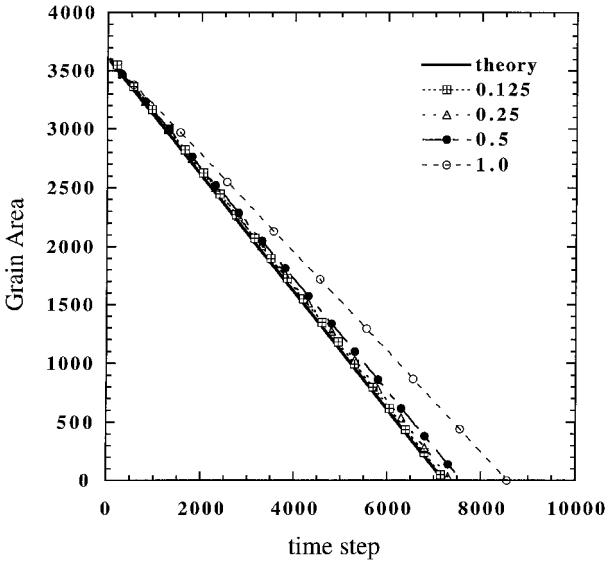

The time dependence of the area of a circular grain embedded in another grain. Comparing the analytical solution with simulations of $\mu = 0{\cdot}125$, $\mu = 0{\cdot}25$, $\mu = 0{\cdot}5$ and $\mu = 1{\cdot}0$.

Fig. 3

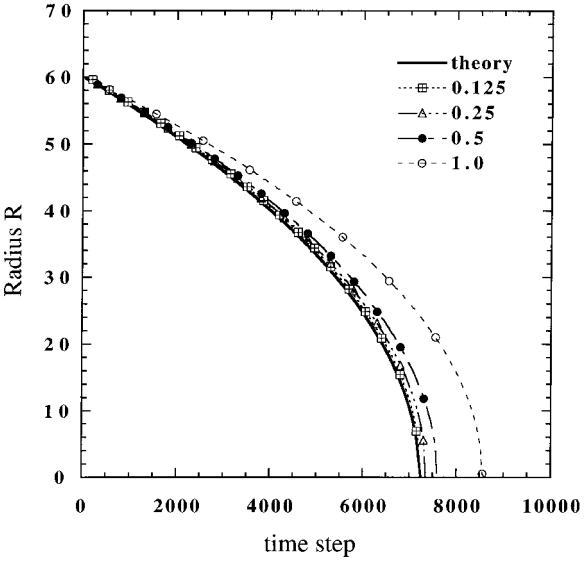

The time dependence of the radius of a circular grain embedded in another grain. Comparing the analytical solution with simulations of $\mu = 0{\cdot}125$, $\mu = 0{\cdot}25$, $\mu = 0{\cdot}5$ and $\mu = 1{\cdot}0$.

Fig. 4

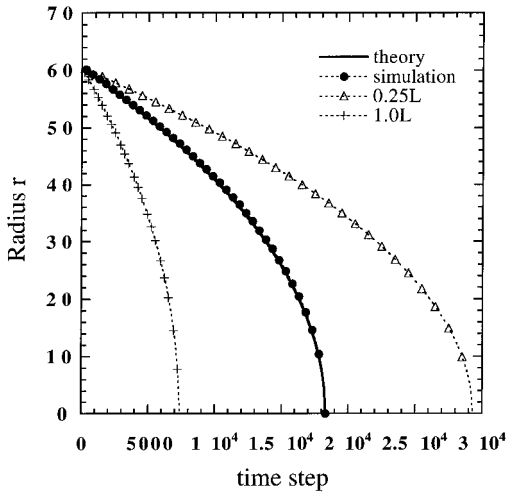

The grain boundary motion with different boundary mobilities. The two dashed lines are theoretical predictions for $L_1 = L_1 = 1{\cdot}0$ and $L_1 = L_1 = 0{\cdot}25$. The solid line is the prediction with $L = 2L_1L_2/(L_1 + L_2)$. The solid dots represent the simulation data with $L_1 = 1{\cdot}0$ and $L_2 = 0{\cdot}25$.

boundary is about 10 grid points, a diffuse grain boundary predicts identical positions and velocities with the sharp-boundary solution. Since the boundary thickness is measured in terms of the number of grid points, we also compared the boundary velocities obtained using two different grid sizes Δx, while keeping k, L, and Δf_0 constant. It is shown that the velocity obtained with a finer grid size agrees well with the analytical solution and further refinement does not change the boundary velocity.

We also compared the numerical simulation results and the analytical solution for the case, $L_1 = 0{\cdot}25$, $L_2 = 1{\cdot}0$, $\mu = 0{\cdot}125$, $\kappa_1 = \kappa_2 = 2{\cdot}0$. These conditions ensure that there are enough grid points to resolve the boundary width. In fig. 4, the two dashed lines are the predictions and simulations with $L_1 = L_2 = 0{\cdot}25$ and $L_1 = L_2 = 1{\cdot}0$ respectively. The solid dots represent the simulation with $L_1 = 0{\cdot}25$, $L_2 = 1{\cdot}0$ and the solid line is the analytical solution from eqn. (12). It can be seen that the diffuse boundary in the simulation behaves exactly the same as that predicted by the analytical solution (eqn. (12)) for the case that $L_1 \neq L_2$.

Another important result obtained from simulations is that the motion of grain boundaries in a single phase system with an isotropic grain boundary energy is indeed independent of the grain boundary energy. In simulations, if there are enough grid points to resolve a grain boundary regime, the velocity is independent of Δf_0, while the grain boundary energy $\sigma_{\alpha\beta}$ does depend on the Δf_0 (eqn. (4)). This result is consistent with eqn. (11) and the result of Allen and Cahn (1979) for antiphase domain boundaries.

§ 5. Discussion

We have shown that a diffuse-interface description of a grain boundary provides almost identical migration velocities to those derived for a sharp interface as long as

there are enough grid points to resolve the boundary width in the numerical simulation, and even if there are not enough grid points, the boundary velocity is still linearly proportional to the curvature. It is quite surprising that this seems to be true even if the grain size is reduced to that comparable to the boundary width. However, it appears not to be the case for solidification (Caginalp and Socolovsky 1989, 1991, 1994, Wheeler, Boettinger and McFadden 1992, Warren and Boettinger 1995), in which numerical simulations based on the diffuse-interface description of the solid–liquid interface produced interface positions and velocities differing significantly from those for a sharp interface if the interface width is too large compared with the crystal size. We would like to emphasize the fundamental differences between the interface motion during solidification and the grain boundary motion during coarsening. In the case of solidification, the driving force for the interface motion is the difference in the chemical potentials within the solid and liquid, which comes from two parts: (1) the bulk free energy difference between the solid and liquid; and (2) the chemical potential difference due to curvatures, the Gibbs–Thomson effect. During solidification, the bulk free energy difference is the dominant driving force for the solid–liquid interface migration. If the interface is too diffuse or the interfacial width is too large, the driving force within the interface region will be reduced and too small compared with that of a sharp interface or an interface with narrower interfacial width. Therefore, the more diffuse the interface is in the numerical simulation, the greater the deviation for the interface velocity from that of a sharp interface prediction. On the other hand, grain boundary motion during grain growth for the case of isotropic grain boundary energy is driven by the mean curvature. In the diffuse-interface field model, the grain boundary regions are those where the gradients $\nabla\eta$ are non-zero. The curvature for a constant η surface is given by the divergence of a unit normal vector to that surface (Allen and Cahn 1979), i.e. $\nabla \cdot \hat{\mathbf{n}}$, where $\hat{\mathbf{n}}$ is the unit vector normal to the surface. The $\nabla \cdot \hat{\mathbf{n}}$ terms are equal to the negative of the mean curvature of surfaces and are implicitly included in the $\nabla^2\eta$ terms. To precisely compute the $\nabla^2\eta$ and $\nabla \cdot \hat{\mathbf{n}}$ terms numerically, there must be enough grid points to describe the grain boundary region. This is the reason why the prediction of a diffuse grain boundary approaches the sharp boundary solution as the width of grain boundary increases for the problems of motion by mean curvatures. The surface tension, which is crucial for the stability of grain boundaries and plays a key role in polycrystalline materials, is proportional to terms $\int(\nabla\eta \cdot \hat{\mathbf{n}})^2 \, \mathrm{d}r$ in the diffuse-interface model (Caginalp and Socolovsky 1991, 1994) and will not be calculated accurately either if there are not enough grid points to resolve the boundary width. It remains to be seen if this is still true for the case of anisotropic grain boundary energies.

For the purpose of modelling microstructural evolution and grain growth kinetics, there are several advantages using the diffuse-interface field kinetic model. First of all, it does not explicitly track the positions of grain boundaries. Secondly, the diffuse-interface field model is a natural description of diffuse boundaries associated with extremely small grains, for example, in nanocrystalline materials. Finally, in the diffuse-interface field model, it is straightforward to describe long-range diffusion, which takes place, for example, during solute segregation and second-phase precipitation at grain boundaries in a polycrystalline material, by coupling the kinetic equations for the orientation field variables with the Cahn–Hilliard diffusion equation for describing the composition evolution (Chen and Fan 1996).

However, as discussed above, in order to match results from the diffuse-interface computation to the analytical solution in the sharp-interface limit, about 10 grid points are necessary for discretizing the ground boundary region. Furthermore, in order to obtain good statistics on grain growth kinetics, several hundred to a few thousand grains at each time step are required. Therefore, accurate spatial discretization of the kinetic equations and realistic simulation of the grain growth kinetics would require very large-scale computer simulations even in two dimensions ($\sim 1000 \times 1000$ grid points), in particular, if uniform grids are employed. Although such simulations are possible in the current generation of computers, they are computationally expensive. However, we have shown above that even if not enough grid points are used to resolve the boundaries, the radius of the circular domain still varies parabolically as a function of time, i.e. the boundary migration velocity is still linearly proportional to the mean curvature, which provides a physical basis for performing simulations with less accurate spatial discretization. Indeed, we recently compared the grain growth simulations with two quite different boundary thicknesses, and we found that there were essentially no differences in the grain growth kinetics including the parabolic growth law for the average grain size as a function of time, the grain size and topological distributions (Fan 1996). The only difference between the results obtained from the two sets of simulations occurs in the rate constants of the parabolic growth laws (k), and from the present analysis, we know precisely the magnitudes of errors in the rate constants due to inaccurate spatial discretization.

§ 6. Conclusions

Based on the diffuse-interface description, a corresponding sharp-interface solution for the grain boundary velocity is derived. In the case of isotropic grain boundary energies, the velocity of grain boundary migration is shown to be linearly proportional to the mean curvature, and is independent of the grain boundary energy, similar to the motion of antiphase domain boundaries as treated by Allen and Cahn. It is shown the velocities of grain boundary migration obtained from a numerical simulation of the grain boundary motion of much wider interfacial region are also proportional to the mean curvature regardless of the numerical accuracy, but their values are identical to those for a sharp grain boundary only if there are enough grid points to resolve the boundary width in the simulation.

Acknowledgments

We gratefully acknowledge the many helpful discussions with H. L. Hu and Q. Wang. The work is supported by the National Science Foundation under the grant number DMR 93-11898 and 96-33719 and the simulations were performed at the Pittsburgh Supercomputing Center.

References

Allen, S. M., and Cahn, J. W., 1979, *Acta metall.*, **27**, 1085.
Atkinson, H. V., 1988, *Acta metall.*, **36**, 469.
Bray, A. J., 1994, *Adv. Phys.*, **43**, 357.
Caginalp, G., and Socolovsky, E., 1991, *J. comput. Phys.*, **95**, 85; 1994, *SIAM J. Sci. Comput.*, **15**, 106.
Chen, L.-Q., 1995, *Scripta metall. mater.*, **32**, 115.
Chen, L.-Q., and Fan, D., 1996, *J. Am. Ceram. Soc.*, **79**, 1163.
Chen, L.-Q., and Yang, W., 1994, *Phys. Rev.* B, **50**, 15 752.

FAN, D., 1996, Ph.D. Thesis, Department of Materials Science and Engineering, Penn State University.
FAN, D., and CHEN, L.-Q., 1997, *Acta metall.*, **45**, 611.
FRADKOV, V. E., 1993, *Physica* D, **66**, 50.
GLAZIER, J. A., 1990, *Phil. Mag.* B, **62**, 615.
WARREN, J. A., and BOETTINGER, W. J., 1995, *Acta metall.*, **43**, 689.
WHEELER, A. A., BOETTINGER, W. J., and MCFADDEN, G. B., 1992, *Phys. Rev.* A, **45**, 7424.